Experimental Activation of Strong Local Passive States with Quantum Information

Nayeli A. Rodríguez-Briones[1,2,*] Hemant Katiyar[3,4] Eduardo Martín-Martínez,[3,5,6] and Raymond Laflamme[3,4,5]

[1]*Department of Chemistry, University of California, Berkeley, California 94720, USA*
[2]*Miller Institute for Basic Research in Science, 468 Donner Lab, Berkeley, California 94720, USA*
[3]*Institute for Quantum Computing, University of Waterloo, Waterloo, Ontario N2L 3G1, Canada*
[4]*Department of Physics and Astronomy, University of Waterloo, Waterloo, Ontario N2L 3G1, Canada*
[5]*Perimeter Institute for Theoretical Physics, 31 Caroline Street North, Waterloo, Ontario N2L 2Y5, Canada*
[6]*Department of Applied Mathematics, University of Waterloo, Waterloo, Ontario N2L 3G1, Canada*

Strong local passivity is a property of multipartite quantum systems from which it is impossible to extract energy locally. Surprisingly, if the strong local passive state displays entanglement, it could be possible to locally activate energy density by adding classical communication between different partitions of the system, through so-called "quantum energy teleportation" protocols. Here, we report both the first experimental observation of local activation of energy density on an entangled state and the first realization of a quantum energy teleportation protocol using nuclear magnetic resonance on a bipartite quantum system.

Introduction.—Methods to extract and transfer energy from physical systems at the quantum scale have been developed recently using tools from quantum information processing and quantum thermodynamics [1–23]. But can these tools allow us to activate energy extraction from quantum systems in which outgoing energy flows are locally blocked [24,25]—or to activate locally hidden energy in entangled ground states? One may be tempted to answer "no," as this would seem to involve activating zero-point energy, which is generally considered impossible. However, we will discuss that the answer to these questions is nuanced and that zero-point energy density can be activated using quantum informational tools.

The quantum states from which it is impossible to extract energy via general local access on a single subsystem receive the name of strong local passive (SLP) states [24–26] (Fig. 1). This distinctive property of strong local passivity is present in a wide range of states, from ground states to thermal states below a critical temperature and even in strongly coupled heat baths in the thermodynamic limit. The necessary and sufficient conditions for this property were presented in Ref. [25].

Strong local passivity provides new insights into the emergent thermodynamic behavior arising from the interplay between entanglement and localization, such as understanding the allowed flows of energy and information within entangled quantum systems. Along these lines, a fundamental question is how and when strong local passivity can be broken. Certainly, finding methods to activate the nondirectly available energy in SLP states can bring fascinating physical scenarios, such as activating entangled ground states. Indeed, in interacting multipartite

quantum systems, the ground state can have regions of positive (and negative) energy density due to its entanglement [27]. However, the corresponding energy is not directly available since any action attempting to extract it directly will only give energy to the system. Could this energy be activated by driving the system differently?

This question was answered by Masahiro Hotta, who showed that, under certain conditions, it is possible to activate strong local passive states by allowing local operations and classical communication (LOCC) to exploit correlations between distant parts of the system [24,28–35]. He introduced the family of protocols known under the general name of quantum energy teleportation (QET), which enables the activation of local energy using informed local operations that depend on the outcome of distant measurements on other sides of the system. Specifically, in
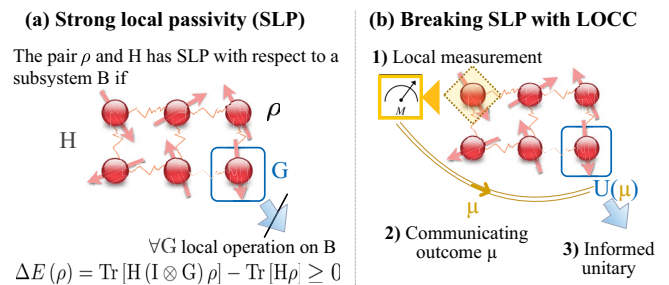

FIG. 1. (a) A quantum state ρ is defined to be strong local passive with respect to a Hamiltonian H and a subsystem if energy cannot be extracted through any direct local quantum operation G applied on the subsystem. (b) Steps for breaking strong local passivity by adding local operations and classical communication (LOCC).

a QET protocol, a local measurement is made on a subsystem (A) far from the subsystem (B) where the energy is blocked. Then, the outcome of this measurement is communicated to B's side. Because of the correlations, this outcome allows us, to some extent, to predict and design an informed local operation to extract the previously inaccessible energy, see Fig. 1. It is important to note that despite the name of the protocol, it does not imply that the energy injected during A's measurement disappears from A's surroundings to appear around B. Indeed, the key feature of the QET protocol is to ensure that the energy extracted comes only from the previously unavailable energy. Thus, for QET it is crucial that the local measurement on A does not raise the energy in B's surroundings—which can be achieved by using measurement operators that commute the interacting Hamiltonian term—and that the protocol must be performed within a time shorter than the energy propagation timescale on the system. Beyond the importance of QET in the activation of passive states, QET has also been suggested to be relevant to understanding a broad range of situations—from the black-hole information loss problem [28,36–38] and violations of energy conditions in quantum field theory in curved spacetimes [39] to technological applications such as local cooling of many-body systems with restricted measurements [12].

However, despite the potential applications of the QET protocol, it had not yet been realized in an experiment. Experimental proposals did exist, for instance, using a semiconductor exhibiting the quantum Hall effect [40], but no actual experiments had been conducted. This Letter presents the first experimental realization of a quantum energy teleportation protocol, demonstrating energy activation in a strong local passive state, in particular, the local activation of zero-point energy density. The experiment was carried out using nuclear magnetic resonance on a system of three qubits in the ground state of an interacting simulated Hamiltonian. The experimental results show energy extraction from a system initially in an SLP state, beyond local and ambient noise, without energy transfer through the system. Our experiment demonstrates the feasibility of the control required for a QET protocol and the first evidence of activation of local zero-point energy density in an entangled ground state under experimental conditions. Furthermore, we present an optimized, fully unitary QET model and an analytical solution for the maximum extractable energy for our system.

We begin by summarizing the minimal QET model [34] to show how it is possible to break strong local passivity to activate regions of an entangled ground state. Then, we present the equivalent fully unitary version of QET implemented in the experiment, followed by the experimental results and conclusions.

Minimal QET model.—Consider two interacting qubits, A and B, with a Hamiltonian that has a nondegenerate fully entangled ground state. An example of such a Hamiltonian is

$$H = H_A + H_B + V, \tag{1}$$

with $H_\nu = -h_\nu \sigma_z^\nu + h_\nu f(h_A, h_B, \kappa)\mathbb{1}$, for $\nu \in \{A, B\}$ and

$$V = 2\kappa \sigma_x^A \sigma_x^B + \frac{4\kappa^2}{h_A + h_B} f(h_A, h_B, \kappa)\mathbb{1}, \tag{2}$$

where h_A, h_B and κ are positive constants, and the function $f(h_A, h_B, \kappa)$ is chosen such that the ground state $|g\rangle$ of the full Hamiltonian has vanishing expectation values for each of its terms ($\langle g|H_A|g\rangle = \langle g|H_B|g\rangle = \langle g|V|g\rangle = 0$) for convenience and without loss of generality. For this Hamiltonian, $f(h_A, h_B, \kappa) = (4\kappa^2/(h_A + h_B)^2 + 1)^{-1/2}$.

This Hamiltonian has a nondegenerate fully entangled ground state

$$|g\rangle = (F_+|00\rangle_{AB} - F_-|11\rangle_{AB})/\sqrt{2}, \tag{3}$$

where $F_\pm = \sqrt{1 \pm f(h_A, h_B, \kappa)}$, satisfying the sufficient conditions to have a family of SLP states (see Ref. [24]). While the total Hamiltonian is a nonnegative operator ($H \geq 0$ since its lowest eigenvalue is 0), H_B and $H_B + V$ allow negative eigenvalues which could yield negative energy density in B's surroundings. A QET protocol can locally activate that energy, as described below.

Minimal QET model, implemented by Alice and Bob:

Step 1: Alice measures subsystem A using a positive operator-valued measure (POVM) with measurement operators $M_A(\mu)$ that commute with the interacting Hamiltonian term ($[M_A(\mu), V] = 0$), to ensure that the energy injected during the measurement does not raise the energy of subsystem B [34,41].

Step 2: Alice communicates the measurement result μ to Bob in a time t_μ shorter than the coupling timescale $t_c \sim 1/\kappa$ to avoid the energy infused in A during the measurement propagates to B during that time.

Step 3: Based on the outcome μ, Bob implements an optimized local unitary on B, $U_B(\mu)$, to extract previously unavailable energy through B (see Fig. 2)

The effect of repeatedly and identically applying the QET protocol to a state ρ can be described by the evolution of the density matrix [34]:

$$\rho_f = \sum_{\mu=\pm 1} U_B(\mu)M_A(\mu)\rho M_A^\dagger(\mu)U_B^\dagger(\mu), \tag{4}$$

where $M_A(\mu)$ is the measurement operator of a POVM on A with outcome μ that commutes with V; and $U_B(\mu)$ is an informed unitary that maximizes the energy extraction depending on the outcome. Then, the amount of energy extracted locally from B on average is given by

$$-\Delta E_B = -\text{Tr}[(H_B + V)\rho_f] \geq 0, \tag{5}$$

since $[M_A(\mu), V] = [M_A(\mu), H_B] = 0$ and given that the expectation value of each term of the Hamiltonian was set
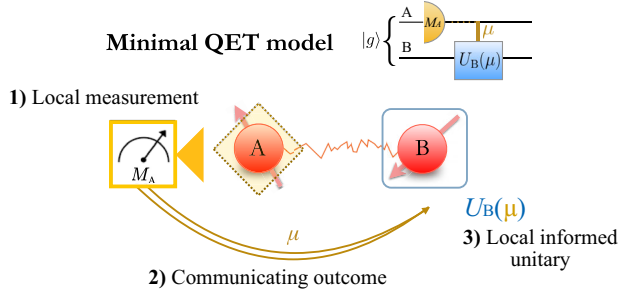
FIG. 2. Minimal QET protocol steps, performed on a pair of qubits initially in a strong local passive state: (1) A local measurement is performed on qubit A using measurement operators $\{M_A\}$ that ensure the energy injected during the measurement remains local to A and does not raise the energy in B's surroundings. (2) The measurement outcome is communicated to B in a time shorter than the energy propagation timescale. (3) Based on this information, a local unitary operation is performed on B to extract energy.
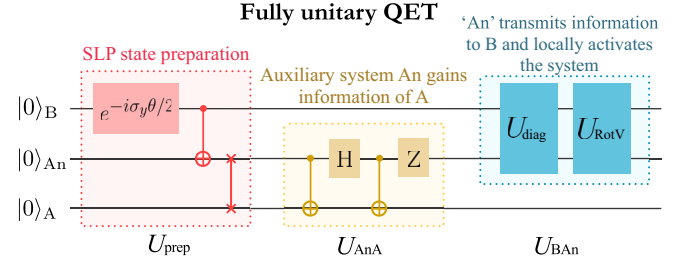

FIG. 3. Fully unitary QET protocol, performed by adding an auxiliary qubit (An) to mediate the measurement of A and transmit information to B. This circuit was optimized to locally activate the passive state given in Eq. (3), of Hamiltonian $H \propto -h_A\sigma_z^A - h_B\sigma_z^B + 2\kappa\sigma_x^A\sigma_x^B$ and $H_{An} \propto \sigma_z^{An}$. See Supplemental Material [44] for the QET protocols' equivalence and details on the experimental implementation.

to zero (see Appendix C3 in [42] and [34] for the detailed calculation). It is important to note that if the measurement outcome is not communicated to B (i.e., having U_B independent of μ), it is impossible to extract energy from subsystem B on average. This underscores the importance of the communication in QET.

From Eq. (5), the amount of extractable energy is bounded by $0 \leq -\Delta E_B \leq -\lambda_{\min}$, where $\lambda_{\min}$ is the most negative eigenvalue of $H_B + V$. This upper bound is tight when the POVMs are proportional to projective operators. In particular, for the ground state of the Hamiltonian in Eq. (1), the maximum amount of extractable energy from subsystem B is

$$(-\Delta E_B)_{\max} = -\sqrt{h_B^2 + 4\kappa^2} + \frac{h_B(h_A + h_B) + 4\kappa^2}{\sqrt{(h_A + h_B)^2 + 4\kappa^2}}, \quad (6)$$

and can be activated by QET, using projection operators of observable σ_x^A. In this case, the average energy injected into A is $E_A = h_A/\sqrt{1 + 4\kappa^2/(h_A + h_B)^2} \geq (-\Delta E_B)_{\max}$. Note that the energy E_A injected into subsystem A remains in that subsystem during the protocol, since the timescale t_μ for transmitting classical communication from A to B is much shorter than the timescale for energy to propagate from A to B (i.e., $t_\mu \ll t_c \sim 1/\kappa$). As a result, the energy extracted corresponds only to the activated energy within the local zero-point energy density.

Experimental implementation.—To perform the protocol using nuclear magnetic resonance (NMR), we designed a fully unitary QET by introducing an auxiliary system to mediate the measurement of A and transmit information to B, as detailed below. The fully unitary version of the QET protocol is equivalent to the minimal QET since the role of a general measurement device can be played by an auxiliary system (An) together with unitary dynamics [43].

This equivalence is proven in Supplemental Material [44]. The equivalence of a fully unitary QET and the minimal QET has been discussed in Refs. [35,39,49].

The experiments were performed on a Bruker Avance III 700 MHz NMR spectrometer, using ^{13}C-labeled transcrotonic acid dissolved in acetone-d6 as the sample. The carbons labeled as $C_1, C_2,$ and C_3 were used as subsystems B, An, and A, respectively [Fig. 4(a)]. The entire experiment took place at an ambient temperature of 298 K. The fully unitary QET protocol consists of the following steps (an overview of the experimental scheme is shown in Fig. 3):

Step 0: Preliminary preparation of the SLP state of Eq. (3). The system starts in the pseudopure state $|000\rangle$ [45], followed by a global unitary U_{prep}. The required unitary consists of a rotation $Y(\theta) = e^{-i\sigma_y\theta/2}$ on qubit B, followed by a CNOT on A and B (with B as the control). The explicit form of $Y(\theta)$ is

$$Y(\theta) = -\frac{1}{\sqrt{2}}\begin{pmatrix} F_+ & F_- \\ -F_- & F_+ \end{pmatrix}, \quad (7)$$

where $F_\pm = \sqrt{1 \pm (h_A + h_B)/\sqrt{4\kappa^2 + (h_A + h_B)^2}}$.

In the experiment, the CNOT gate was not directly implemented between subsystems A and B for state preparation, but instead decomposed into two gates acting on subsystems A-An and B-An to improve the state preparation fidelity in our concrete system (see Fig. 3). This is because the J-coupling values of the spin pairs A-An and B-An are higher than the J coupling of the A-B pair [50], as shown in Fig. 4. Refer to Supplemental Material [44] for a more detailed physical explanation.

Step 1: Alice gains information about qubit A through an auxiliary qubit An by applying a joint unitary U_{AnA} on both qubits. The optimal unitary U_{AnA} corresponds to the one that maximizes the mutual information between A and An, subject to the condition $[U_{\text{AnA}}, V] = 0$ (so it does not raise the energy of B's surroundings). For a pair of qubits in a product state, an optimal unitary is

(a) Transcrotonic acid molecule

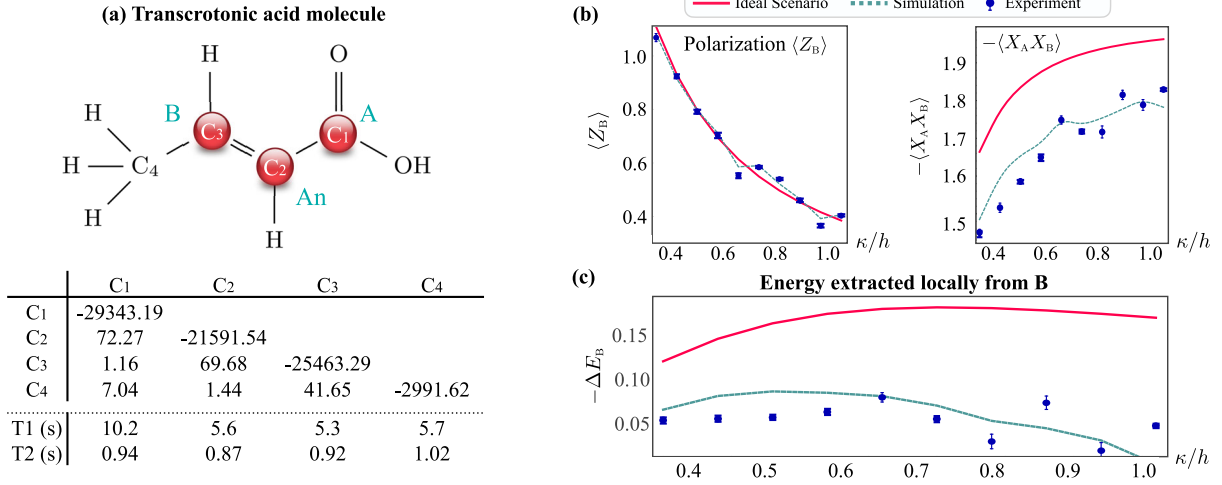|	C_1	C_2	C_3	C_4
C_1	-29343.19			
C_2	72.27	-21591.54		
C_3	1.16	69.68	-25463.29	
C_4	7.04	1.44	41.65	-2991.62
T1 (s)	10.2	5.6	5.3	5.7
T2 (s)	0.94	0.87	0.92	1.02

FIG. 4. (a) System set up in a transcrotonic acid molecule. The table shows the Hamiltonian parameters: the diagonal values correspond to the chemical shifts, and off-diagonal elements correspond to the J-coupling values, all in Hz. The relaxation timescales, T_1 and T_2 are shown in the bottom. (b) Experimental results: expectation values $-\langle X_A X_B \rangle$ and $\langle Z_B \rangle$ after implementing the protocol. (c) Energy extracted $-\Delta E_B$, plotted against the coupling strength κ/h between systems A and B, for $h_B = 0.4\, h_A$ and fixing $h_A = h = 1$.

$$U_{\text{AnA}} = \frac{1}{\sqrt{2}} \begin{pmatrix} 1 & 0 & 0 & 1 \\ 0 & 1 & 1 & 0 \\ 0 & -1 & 1 & 0 \\ -1 & 0 & 0 & 1 \end{pmatrix}. \qquad (8)$$

The explicit gates for this unitary are shown in Fig. 3.

Step 2: Alice sends the auxiliary qubit An to Bob in a time t_μ shorter than the coupling timescale to avoid that energy infused on A propagates to B during the protocol.

Step 3: Finally, Bob implements a joint unitary U_{BAn} on B and An to extract energy from the system by acting locally on B.

For the experiment, we optimized U_{BAn} to achieve the upper bound $(-\Delta E_B)_{\max}$, given by Eq. (6), obtaining

$$U_{\text{BAn}} = U_{\text{Rot}V} U_{\text{diag}}, \quad \text{where}$$

$$U_{\text{Rot}V} = \frac{1}{\sqrt{2}} \begin{pmatrix} F_{2_+} & F_{2_-} & 0 & 0 \\ 0 & 0 & -F_{2_+} & F_{2_-} \\ 0 & 0 & F_{2_-} & F_{2_+} \\ -F_{2_-} & F_{2_+} & 0 & 0 \end{pmatrix},$$

$$U_{\text{diag}} = \frac{1}{\sqrt{2}} \begin{pmatrix} 0 & F_+ & F_- & 0 \\ F_- & 0 & 0 & -F_+ \\ F_+ & 0 & 0 & F_- \\ 0 & -F_- & F_+ & 0 \end{pmatrix},$$

with $F_{2_\pm} = \sqrt{1 \pm h_B / \sqrt{(h_B^2 + 4\kappa^2)}}$.

The gates for the protocol, shown in Fig. 3, were implemented using GRAPE pulses [46] with a slight modification to incorporate the technique described in Ref. [51], resulting in the designing of smooth radio frequency (rf) pulses with theoretical fidelity over 0.998 and robust against small imperfections in rf power.

The unitaries U_{AnA} and U_{BAn} were performed in $\simeq 10$ ms and 4 ms, respectively. Thus, the total time from the beginning of Step 1 to the activation of energy was $t_\mu \simeq 14$ ms. This time fulfills the condition for QET: $t_\mu \ll t_c$, where $t_c \sim 1/J_{\text{AB}} = (1.16 \text{ Hz})^{-1}$ for the transcrotonic molecule. Namely, t_μ is much shorter than the time it would take for energy to propagate from A to B.

The amount of extracted energy was calculated using the experimental results of the expectation values for the interaction term operator $-\langle X_A X_B \rangle$ and B's local Hamiltonian operator $\langle Z_B \rangle$, which were measured directly at the end of the circuit. The experimental results are plotted in Fig. 4, as a function of the coupling strength between A and B. The curves for the ideal scenario show the expected outcome of implementing the circuit perfectly, without any decoherence. On the other hand, the curves for the simulation were generated using optimized GRAPE pulses that take decoherence into account. The decoherence simulation assumes that the environment is Markovian, the qubits relax independently, and the dissipator commutes with the total Hamiltonian for the time discretization in GRAPE pulses ($\Delta t = 2$ μs). These assumptions simplify the implementation of master equations for each time step, the evolution under the propagator of the GRAPE pulses, and the dissipator. All of the experimental results give energy extraction, providing the first evidence of activation of a strong local passive state under experimental conditions. The discrepancy between the simulation and the experiment is due to the decoherence assumptions

and the transfer function of the spectrometer, which executes the GRAPE pulses slightly differently than assumed. The error bars shown represent only the statistical error of the experiment.

Numerical tests show that the protocol is stable under some uncertainty in the local Hamiltonians. To study this sensitivity, we added perturbations in the local parts of the Hamiltonian while performing the optimized QET protocol for the nonperturbed case. We considered perturbed local Hamiltonians of the form $h_\nu \propto (1 + \epsilon)h_\nu \sigma_z^\nu + h_\nu f(h_A, h_B, \kappa)\mathbb{1}$. We found that if the parameter ϵ (quantifying the relative difference between the Hamiltonian assumed and the actual Hamiltonian) is small, $\epsilon \leq 0.3$, then the relative impact of the error in the implementation of the protocol is neglectable.

Conclusions.—We presented the first experimental activation of strong local passive states and the first experimental demonstration of a quantum energy teleportation (QET) protocol proposed by Hotta [31,32]. Furthermore, our experiment confirms for the first time that the presence of entanglement in a ground state allows for local zero-point energy density activation without energy transfer through the system.

We show experimental energy extraction from a bipartite system, initially in a strong local passive state but activated through local operations and communication, using a quantum energy teleportation protocol. We designed a fully unitary quantum energy teleportation protocol optimized to maximize the energy extraction under the constraints of our experimental setup. The experiment was carried out using nuclear magnetic resonance, demonstrating that the required control for a quantum energy teleportation protocol can be achieved in realistic experimental scenarios. Furthermore, the optimization of the fully unitary QET demonstrates that the maximum possible amount of activated energy can only be achieved when the measurement device and the measured subsystem gain full mutual information and the measurement outcome is transmitted to the target subsystem.

The QET protocol has the potential to be a valuable tool for a fundamental understanding of quantum thermodynamics and for quantum technologies. On the fundamental side, QET helps understand quantum fluctuations and their role in fundamental scenarios, from quantum field theory in curved spacetimes to quantum thermodynamics: from black hole physics [28,36–38] to violations of energy conditions in quantum field theory in curved spacetimes [39]. On the technological side, it has been proposed as a method for improving the purity locally by exploiting interaction-induced correlations in algorithmic cooling protocols [12]. Another application appears in scenarios where SLP can potentially impose restrictions on thermodynamic tasks and the regime in which some quantum machines can perform, especially those that rely on energy exchange through

local quenching and/or pulses that are fast compared to the dynamics of the system, for example, in Refs. [52–55]. This experimental demonstration of QET for the first time paves the way for the experimental implementation and exploration of these protocols in controlled quantum systems.

[*]nayelongue@berkeley.edu

[1] N. Brunner, N. Linden, S. Popescu, and P. Skrzypczyk, Phys. Rev. E **85**, 051117 (2012).

[2] N. Linden, S. Popescu, and P. Skrzypczyk, Phys. Rev. Lett. **105**, 130401 (2010).

[3] A. Levy and R. Kosloff, Phys. Rev. Lett. **108**, 070604 (2012).

[4] P. O. Boykin, T. Mor, V. Roychowdhury, F. Vatan, and R. Vrijen, Proc. Natl. Acad. Sci. U.S.A. **99**, 3388 (2002).

[5] L. J. Schulman and U. V. Vazirani, in *Proceedings of the 31st Annual ACM Symposium on Theory of Computing STOC 99* (1999), p. 322, 10.1145/301250.301332.

[6] J. M. Fernandez, S. Lloyd, T. Mor, and V. Roychowdhury, Int. J. Quantum. Inform. **02**, 461 (2004).

[7] L. J. Schulman, T. Mor, and Y. Weinstein, Phys. Rev. Lett. **94**, 120501 (2005).

[8] L. J. Schulman, T. Mor, and Y. Weinstein, SIAM J. Comput. **36**, 1729 (2007).

[9] O. W. Sørensen, J. Magn. Reson. (1969) **86**, 435 (1990).

[10] O. W. Sørensen, J. Magn. Reson. (1969) **93**, 648 (1991).

[11] D. K. Park, N. A. Rodriguez-Briones, G. Feng, R. Rahimi, J. Baugh, and R. Laflamme, in *Electron Spin Resonance Based Quantum Computing*, edited by T. Takui, L. Berliner, and G. Hanson (Springer, New York, 2016), pp. 227–255, 10.1007/978-1-4939-3658-8_8.

[12] N. A. Rodríguez-Briones, E. Martín-Martínez, A. Kempf, and R. Laflamme, Phys. Rev. Lett. **119**, 050502 (2017).

[13] N. A. Rodríguez-Briones and R. Laflamme, Phys. Rev. Lett. **116**, 170501 (2016).

[14] E. Köse, S. Çakmak, A. Gençten, I. K. Kominis, and O. E. Müstecaplıoğlu, Phys. Rev. E **100**, 012109 (2019).

[15] N. A. Rodríguez-Briones, J. Li, X. Peng, T. Mor, Y. Weinstein, and R. Laflamme, New J. Phys. **19**, 113047 (2017).

[16] Á. M. Alhambra, M. Lostaglio, and C. Perry, Quantum **3**, 188 (2019).

[17] W. Niedenzu, V. Mukherjee, A. Ghosh, A. G. Kofman, and G. Kurizki, Nat. Commun. **9**, 165 (2018).

[18] T. D. Kieu, Phys. Rev. Lett. **93**, 140403 (2004).

[19] H. T. Quan, Y.-x. Liu, C. P. Sun, and F. Nori, Phys. Rev. E **76**, 031105 (2007).

[20] J. Cotler, S. Choi, A. Lukin, H. Gharibyan, T. Grover, M. E. Tai, M. Rispoli, R. Schittko, P. M. Preiss, A. M. Kaufman, M. Greiner, H. Pichler, and P. Hayden, Phys. Rev. X **9**, 031013 (2019).

[21] M. P. Zaletel, A. Kaufman, D. M. Stamper-Kurn, and N. Y. Yao, Phys. Rev. Lett. **126**, 103401 (2021).

[22] F. Clivaz, R. Silva, G. Haack, J. B. Brask, N. Brunner, and M. Huber, Phys. Rev. Lett. **123**, 170605 (2019).

[23] M. Gluza, J. Sabino, N. H. Y. Ng, G. Vitagliano, M. Pezzutto, Y. Omar, I. Mazets, M. Huber, J. Schmiedmayer, and J. Eisert, PRX Quantum **2**, 030310 (2021).

[24] M. Frey, K. Funo, and M. Hotta, Phys. Rev. E **90**, 012127 (2014).

[25] A. M. Alhambra, G. Styliaris, N. A. Rodríguez-Briones, J. Sikora, and E. Martín-Martínez, Phys. Rev. Lett. **123**, 190601 (2019).

[26] The strong local passive states are also called CP-local passive states [25], referring to the fact that energy cannot be extracted under any local completely positive (CP) trace-preserving map, the most general type of local access.

[27] In general, the entangled ground state of a multipartite quantum system possesses regions of positive (and negative) energy density, depending on the expectation values of the Hamiltonian terms that have support in that particular region.

[28] M. Hotta, Phys. Rev. D **81**, 044025 (2010).

[29] M. R. Frey, K. Gerlach, and M. Hotta, J. Phys. A **46**, 455304 (2013).

[30] M. Hotta, J. Matsumoto, and G. Yusa, Phys. Rev. A **89**, 012311 (2014).

[31] M. Hotta, J. Phys. Soc. Jpn. **78**, 034001 (2009).

[32] M. Hotta, Phys. Lett. A **372**, 5671 (2008).

[33] J. Trevison and M. Hotta, J. Phys. A **48**, 175302 (2015).

[34] M. Hotta, Phys. Lett. A **374**, 3416 (2010).

[35] G. Verdon-Akzam, Ph.D. thesis, University of Waterloo, Canada, 2017.

[36] S. L. Braunstein and A. K. Pati, Phys. Rev. Lett. **98**, 080502 (2007).

[37] P. Hayden and J. Preskill, J. High Energy Phys. 09 (2007) 120.

[38] A. Hosoya and A. Carlini, Phys. Rev. D **66**, 104011 (2002).

[39] N. Funai and E. Martín-Martínez, Phys. Rev. D **96**, 025014 (2017).

[40] G. Yusa, W. Izumida, and M. Hotta, Phys. Rev. A **84**, 032336 (2011).

[41] A POVM with measurement operators $M_A(\mu)$ that commute with H_B and V (i.e., $[H_B, M_A(\mu)] = [V, M_A(\mu)] = 0$) will not raise the energy in B since the expectation values of the Hamiltonian terms that have support on B's surroundings do not change. Namely, $\mathrm{Tr}[H_B M_A(\mu)|g\rangle\langle g|M_A^\dagger(\mu)] = \mathrm{Tr}[H_B|g\rangle\langle g|] = 0$, similarly for V. See Appendix C3 in [42] and [34] for detailed calculations.

[42] N. A. Rodríguez-Briones, Ph.D. thesis, University of Waterloo, Canada, 2020.

[43] M. A. Nielsen and I. Chuang, *Quantum Computation and Quantum Information* (Cambridge Univ. Press, Cambridge, 2011).

[44] See Supplemental Material at http://link.aps.org/supplemental/10.1103/PhysRevLett.130.110801 for details of how the minimal QET protocol can be implemented in a fully unitary version using an auxiliary system; and a description of the experimental implementation, which includes Refs. [43,45–48].

[45] D. G. Cory, M. D. Price, and T. F. Havel, Physica (Amsterdam) **120D**, 82 (1998).

[46] N. Khaneja, T. Reiss, C. Kehlet, T. Schulte-Herbruggen, and S. J. Glaser, J. Magn. Reson. **172**, 296 (2005).

[47] M. H. Levitt, *Spin Dynamics: Basics of NMR* (John Wiley & Sons, New York, 2013).

[48] E. M. Fortunato, M. A. Pravia, N. Boulant, G. Teklemariam, T. F. Havel, and D. G. Cory, J. Chem. Phys. **116**, 7599 (2002).

[49] G. Verdon-Akzam, E. Martín-Martínez, and A. Kempf, Phys. Rev. A **93**, 022308 (2016).

[50] The stronger the coupling between spins, the higher the fidelity of a global unitary on both. Direct coupling between B and A is smaller and would result in a longer gate time. For comparison, a CNOT gate between B and A would take roughly 431 ms while using An to mediate the gate is around 26 ms.

[51] J. P. S. Peterson, R. S. Sarthour, and R. Laflamme, Phys. Rev. Appl. **13**, 054060 (2020).

[52] R. Gallego, A. Riera, and J. Eisert, New J. Phys. **16**, 125009 (2014).

[53] M. Perarnau-Llobet, H. Wilming, A. Riera, R. Gallego, and J. Eisert, Phys. Rev. Lett. **120**, 120602 (2018).

[54] D. Gelbwaser-Klimovsky and A. Aspuru-Guzik, J. Phys. Chem. Lett. **6**, 3477 (2015).

[55] D. Newman, F. Mintert, and A. Nazir, Phys. Rev. E **95**, 032139 (2017).